SOME NEW ALGORITHMS FOR SOLVING THE COUPLED ELECTRON-PHOTON TRANSPORT PROBLEMS BY THE DISCRETE-ORDINATES METHOD

A. M. Voloschenko and S. V. Gukov
Keldysh Institute of Applied Mathematics, Moscow, 125047, Miusskaya Sq., 4, Russia
volosch@kiam.ru , gukov@pool-7.ru

ABSTRACT

The coupled electron-photon multigroup cross-section generating code CEPXS from package CEPXS/ONELD [1-3] has been successfully adapted for the use with the current versions of 1D and 2D transport codes ROZ-6.5 and KASKAD-S-2, where the possibility of the use of nodal schemes, direct treatment of the continuous slowing-down (CSD) term and the continuous scattering term (the last option is available only for ROZ-6.5) of the Boltzmann-Fokker Planck (BFP) equation is implemented. The new cross-sections interface, based on the use of the lower block triangular (LBT) form of the multigroup scattering matrix that arises if the same energy mesh is used both for photons and electrons, and the standard "by particle" sequence of groups in a coupled electron-photon cross-section file is changed to "by energy" organized sequence of groups, is proposed. It gives the possibility to optimize the upscattering iteration strategy in solving cascade problems. Some additional improvements both in calculation of the uncollided part of radiation from monodirectional sources and accelerating inner iterations convergence are also discussed. A few numerical examples are given.

1. INTRODUCTION

An indirect treatment of the CSD and continuous scattering terms of the BFP equation gives a possibility of the use of standard S_n codes for solving charged particle transport problems. This approach is used in the CEPXS/ONELD package [1-3] for solving 1D coupled electron-photon transport problems. But in some problems, for example, in pencil beam problems [4], the additional approximations, typically used in this approach to transform the system of differencing equations to the form that can be solved by standard S_n codes, generate essential computational errors.

The direct treatment of the CSD and continuous scattering terms of the BFP equation seems more adequate. It essentially increases both the class of possible differencing schemes that can be used for approximation of these terms and algorithms that can be applied to solve the system of equations that arises as a result of these approximations, but requires some additional modifications to be implemented in S_n codes used.

To make the coupled electron-photon multigroup cross-section generating code CEPXS more applicable for the use together with the BFP S_n codes, two new options, based on "Monte-Carlo" option of CEPXS [5], have been implemented in the adapted version of this code, called CEPXS-BFP: *"Sn-CSD"* option, where the CSD operator is treated directly, but the continuous-scattering operator is treated indirectly in the P_L approximation, and *"Sn-BFP"* option, where both the CSD and continuous-scattering operators of BFP equation are treated directly. In *"Sn-BFP"* option both the restricted

stopping power for group boundaries and averaged by group value of the restricted momentum transfer are written to the output cross-section matrix. The third new option, implemented in CEPXS-BFP, is *"Sn-indirect"* option. It is nearly identical with standard CEPXS option with indirect treatment both the CSD and continuous-scattering operators, used by ONEDANT-LD code, but the header cards in output file have been changed to make one's more convenient for the use by cross-section preprocessor ARVES-2 that transforms cross-section matrices, prepared in the ANISN format, to more economical FMAC-M format, used by ROZ-6.5 and KASKAD-S-2 transport codes those are the current versions of codes [6, 7].

The organization of the paper is as follows. In Sec. 2 the new cross-section interface developed to optimize upscattering iterations is described. In Sec. 3 the approximations used to solve the BFP equation in an example of the plane geometry case are outlined. In Sec. 4 the possibilities of the use of the nodal schemes implemented in ROZ-6.5 code for solving the BFP equation by an indirect approach are briefly discussed. The problem of acceleration of inner iterations convergence is discussed in Sec. 5. Some numerical examples those demonstrate performance of used algorithms are presented in Sec. 6, and, finally, conclusions are given.

2. CROSS-SECTION INTERFACE FOR SOLVING CASCADE PROBLEMS

In solving coupled electron-photon problems it is possible essentially decrease computational times by rearranging group sequence and upscattering iteration cycles if the same energy mesh is used for both electrons and photons. Indeed, if we go from the standard “by particle” sequence of the groups in a coupled electron-photon cross-section file

$$1e,\ 2e,\ldots,\ Qe,1\gamma,\ 2\gamma,\ldots,\ Q\gamma,$$

where Q is the number of electron (photon) groups, to the “by energy” organized sequence of the groups

$$1e,\ 1\gamma,\ 2e,\ 2\gamma,\ldots,\ Qe,\ Q\gamma,$$

multigroup scattering matrix transforms to the lower block triangular (LBT) form

$$\begin{array}{ccccccc}
1e\to 1e & 1\gamma\to 1e & 0 & 0 & 0 & 0 & \ldots \\
1e\to 1\gamma & 1\gamma\to 1\gamma & 0 & 0 & 0 & 0 & \ldots \\
1e\to 2e & 1\gamma\to 2e & 2e\to 2e & 2\gamma\to 2e & 0 & 0 & \ldots \\
1e\to 2\gamma & 1\gamma\to 2\gamma & 2e\to 2\gamma & 2\gamma\to 2\gamma & 0 & 0 & \ldots \\
1e\to 3e & 1\gamma\to 3e & 2e\to 3e & 2\gamma\to 3e & 3e\to 3e & 3\gamma\to 3e & \ldots \\
1e\to 3\gamma & 1\gamma\to 3\gamma & 2e\to 3\gamma & 2\gamma\to 3\gamma & 3e\to 3\gamma & 3\gamma\to 3\gamma & \ldots \\
\ldots & \ldots & \ldots & \ldots & \ldots & \ldots & \ldots
\end{array}$$

In this case the upscattering iteration cycle for the full (and huge) multigroup scattering matrix can be changed to a "by-block" upscattering cycles, the source for a calculated block from upper blocks can be calculated only ones and stored in a memory, etc.

Really, due to the energy conservation in cascade processes the created particles have energy that is less than the energy of an input particle. If positrons are also included in the coupled cross-section file, the LBT structure is partially destroyed due the annihilation. But in this case we also have achieved computational gain. The similar approach is applicable in solving hadron cascade problems [4, 8]. Practically, the use of the LBT scattering matrices gives a multifold computational gain that increases with increasing of the order of P_L approximation, number of groups and particle types used.

3. NUMERICAL ALGORITHM FOR SOLVING THE BFP EQUATION

Electron transport can be well treated by means of the BFP equation [9]. The BFP equation uses the Bolzmann scattering integral to treat the large-angle (sufficiently smooth or regular) component of scattering and the differential Fokker-Plank operator to approximate the forward-peaked or "singular" component of scattering. The BFP equation can be written as follows:

$$-\frac{\partial}{\partial E}\left[\beta(\vec{r},E)\psi\right]-T(\vec{r},E)\left\{\frac{\partial}{\partial\mu}\left[(1-\mu^2)\frac{\partial\psi}{\partial\mu}\right]+\frac{1}{1-\mu^2}\frac{\partial^2\psi}{\partial\varphi^2}\right\}+(\vec{\Omega}\vec{\nabla})\psi+\sigma_t(\vec{r},E)\psi(\vec{r},\mu,\varphi,E)=$$

$$=\int_0^\infty dE'\int_0^{2\pi}d\varphi'\int_{-1}^{+1}d\mu'\sigma_s(\vec{r},E'\to E,\mu_s)\psi(\vec{r},\mu',\varphi',E')+F(\vec{r},\mu,\varphi,E)\,. \qquad (1)$$

$$\mu_s=\mu'\mu+\left[\left(1-\mu'^2\right)\left(1-\mu^2\right)\right]^{1/2}Cos(\varphi'-\varphi)\,,\quad \mu=Cos\theta=(\vec{\Omega}\vec{n}_z)\,,\quad \mu'=Cos\theta'=(\vec{\Omega}'\vec{n}_z)\,.$$

The first two operators in this equation are the Fokker-Planck operators. The energy operator is known as the continuous slowing-down (CSD) operator, and the angular operator is known as the continuous-scattering operator. In Eq. (1) $\beta(E)$ is the restricted stopping power, $T(E)=\alpha(E)/2$, where $\alpha(E)$ is the restricted momentum transfer [5]:

$$\beta(E)=\int_0^E 2\pi\int_{-1}^1\sigma_{\sin g}(E\to E',\mu_s)(E-E')d\mu_s dE'\,,\ \alpha(E)=\int_0^E 2\pi\int_{-1}^1\sigma_{\sin g}(E\to E',\mu_s)(1-\mu_s)d\mu_s dE'\,, \qquad (2)$$

where $\sigma_{\sin g}(E\to E',\mu_s)$ is the *singular component* of scattering cross-section. In Eq. (1) $\sigma_t(E)$ and $\sigma_s(E'\to E)$ are total cross-section and the *regular part* of scattering cross-section [9, 5], μ_s is the scattering angle cosine, and F is a given inhomogeneous source. The suitable boundary conditions should be also added to Eq. (1).

The main features of the method used for solving the BFP equation with direct treatment both the CSD and continuous scattering terms can be discussed in an example of plane geometry case

$$\frac{\partial}{\partial E}\left[\beta\psi\right]-T\frac{\partial}{\partial\mu}\left[(1-\mu^2)\frac{\partial\psi}{\partial\mu}\right]+\mu\frac{\partial\psi}{\partial x}+\sigma_t\psi(x,\mu,E)=S(x,\mu,E)\,. \qquad (3)$$

The balance equation is obtained by integrating of Eq. (3) over a cell $\left[E_{q+1/2},E_{q-1/2}\right]\times\left[x_{i-1/2},x_{i+1/2}\right]\times\left[\mu_{m-1/2},\mu_{m+1/2}\right]$, where $E_{q\pm1/2}$ are the q-th group boundaries $\left(E_{q+1/2}<E_{q-1/2}\right)$, $q=1,\ldots,Q$; $i=1,\ldots,I$; $m=1,\ldots,M$, and the use of the second order of accuracy scheme for approximation the continuous scattering term [10]

$$\left(1-\mu^2\right)\frac{\partial\psi}{\partial\mu}|_{\mu=\mu_{m-1/2}}=2\alpha_{m-1/2}\frac{\psi_m-\psi_{m-1}}{\mu_m-\mu_{m-1}},\qquad \left(1-\mu^2\right)\frac{\partial\psi}{\partial\mu}|_{\mu=\mu_{m+1/2}}=2\alpha_{m+1/2}\frac{\psi_{m+1}-\psi_m}{\mu_{m+1}-\mu_m}\,. \qquad (4)$$

Finally, we receive

$$\frac{V}{\Delta E}\left(\beta^+\psi_E^+-\beta^-\psi_E^-\right)+|\mu|\left(\psi_x^+-\psi_x^-\right)+\bar{\sigma}V\psi=VS\,,\quad S_m=\sum_{l=0}^{L}\frac{2l+1}{4\pi}\sigma_{s,l}^{reg}P_l\left(\mu_m\right)\phi_l+\sum_{m'=1}^{M}T_{m,m'}\psi_{m'}+F_m\,, \qquad (5)$$

where

$$\alpha_{m+1/2}-\alpha_{m-1/2}=-w_m\mu_m\,,\qquad \alpha_{1/2}=\alpha_M=0\,,\qquad m=1,..,M\,, \qquad (6)$$

$$V_i=x_{i+1/2}-x_{i-1/2}\,,\quad w_m=\mu_{m+1/2}-\mu_{m-1/2}\,,\quad \psi^{\pm}=\begin{cases}\psi_{i\pm1/2,m,q}\,,\ \mu_m>0\\ \psi_{i\mp1/2,m,q}\,,\ \mu_m<0\end{cases}\,,\quad \phi_l=2\pi\sum\nolimits_m w_m P_l\left(\mu_m\right)\psi_m$$

$$\psi^{\pm}_{E,q} = \Delta E_q \psi_{i,m,q\pm1/2}\,,\quad \beta^{\pm} = \beta(E_{q\pm1/2})\,,\quad \Delta E_q = E_{q-1/2} - E_{q+1/2}\,,\quad \psi^{-}_{E,q+1} = \left(\Delta E_{q+1} \big/ \Delta E_q\right)\psi^{+}_{E,q}\,,\quad \psi^{-}_{E,q=1} = 0\,,$$

$$T_{m,m'} = T\begin{pmatrix} \lambda_0 - \overline{B}_1 & \overline{C}_1 & 0 & \cdot \\ \overline{A}_2 & \lambda_0 - \overline{B}_2 & \overline{C}_2 & \cdot \\ 0 & \overline{A}_3 & \lambda_0 - \overline{B}_3 & \cdot \\ \cdot & \cdot & \cdot & \cdot \end{pmatrix}, \qquad \begin{aligned} &\overline{\sigma} = \sigma_t + \sigma^{FP}\,, \\ &\sigma^{FP} = T\lambda_0\,, \\ &\lambda_0 = \max_m\left(\overline{B}_m\right) \end{aligned} \tag{7}$$

$$\overline{A}_m = \frac{2\alpha_{m-1/2}}{w_m\left(\mu_m - \mu_{m-1}\right)}\,,\quad \overline{C}_m = \frac{w_{m+1}}{w_m}\overline{A}_{m+1}\,,\quad \overline{B}_m = \overline{A}_m + \overline{C}_m\,, \tag{8}$$

In Eq. (5) $\sigma^{reg}_{s,l}$ = scattering moments of regular component of scattering; ϕ_l = angular flux moments; $\overline{\sigma}$ = effective total cross-section; F_m = given group source; $\psi^q_m = \int_{E_{q+1/2}}^{E_{q-1/2}} \psi_m(E)dE$ = angular flux for group q and angular direction μ_m. The choice of λ_0 in Eq. (7) ensures positivity of diagonal elements of matrix $T_{m,m'}$. In this case all elements of $T_{m,m'}$ are nonnegative.

In spatial and energy variables x and E the WDD auxiliary equations are used

$$\psi^{+}_x = (1+P_x)\psi - P_x\psi^{-}_x\,,\quad \psi^{+}_E = (1+P_E)\psi - P_E\psi^{-}_E\,,\quad 0 \le P_x, P_E \le 1\,. \tag{9}$$

The weighting coefficients P_x and P_E in auxiliary equations (9) can be calculated by means of the adaptive WDD (AWDD) scheme [11]. In this scheme the weighting coefficients are defined as a result of estimation of flux gradients for every variable x and E. The AWDD scheme ensures positivity and an acceptable (and adjustable) level of monotonicity of calculated fluxes together with conservation of the high level of accuracy in calculation of integral quantities, peculiar to the DD scheme. It is also important that the AWDD scheme does not destroy inner iterations convergence. In ROZ-6.5 the following variant of the AWDD scheme is used. First, the cell is calculated by means of the DD scheme with $P_E = P_x = 1$. Next, by formula

$$P_E = \begin{cases} 1, & U_E \le U^0_E \\ U^0_E \big/ U_E, & U_E > U^0_E \end{cases}\,,\qquad U^0_E = \frac{\beta^-}{\beta^- + \beta^+} = 1 - \delta_E\,,\qquad U_E = b_E\left|u_E\right|\,,\qquad u_E = \frac{\psi^-_E - \psi}{\psi}\,, \tag{10}$$

where $b_E \ge 1$ is the monotonization parameter in energy variable E, the weight P_E is calculated. If $P_E < 1$ then the cell is recalculated with weight P_E in energy variable. Next, by formula

$$P_x = \begin{cases} 1, & U_x \le U^0_x \\ U^0_x \big/ U_x, & U_x > U^0_x \end{cases}\,,\qquad U^0_x = 0.5\,,\qquad U_x = b_x\left|u_x\right|\,,\qquad u_x = \frac{\psi^-_x - \psi}{\psi}\,, \tag{11}$$

where $b_x \ge 1$ is the monotonization parameter in spatial variable x, the weight P_x is calculated. Standard choice of monotonization parameters in ROZ-6.5 is: $b_E = b_x = 2$. The new variant of the AWDD scheme with iterative refinements of the weighting coefficients is also available in ROZ-6.5.

4. INDIRECT TREATMENT OF THE CONTINUOUS SLOWING-DOWN AND CONTINUOUS SCATTERING TERMS

To avoid working with the three-diagonal scattering matrices, the continuous scattering term can be treated in the P_L approximation [12]. In this case the total and scattering cross-sections are modified

$$\sigma^q_{t,CSD} = \sigma^q_{t,BFP} + T^q L\left(L+1\right)\,,\ \sigma^{q\to q}_{sl,CSD} = \sigma^{q\to q}_{sl,BFP} + T^q\left[L\left(l+1\right) - l\left(l+1\right)\right]\,,\ l = 0,1,\ldots,L\,,\ L = M-1\,. \tag{12}$$

Of course, positivity of scattering is not ensured in this case.

To avoid working with direct treatment of the CSD term, the downscattering that is a δ-function in angle is treated in the P_L approximation. Suppose the DD scheme auxiliary equation is used in energy variable

$$\psi_{q+1/2} = \left(2\psi^q \big/ \Delta E^q\right) - \psi_{q-1/2}\,. \tag{13}$$

After substitution auxiliary equation (13) and similar equation for $\psi_{q-1/2}$ in the balance Eq. (5), we obtain

$$\ldots + \tilde{\sigma}_t^q V\psi^q = V(S^q + \sigma_\beta^{q-1\to q}\psi^{q-1} + \sigma_\beta^{q-2\to q}\psi^{q-2} + \ldots)\,, \tag{14}$$

The terms those are $\sim\psi^{q-1}$, ψ^{q-2},… in the right-hand side of Eq. (14) can be interpreted as the yield of diagonal scattering matrices from previous energy groups. Using the well-known properties of δ-function and additionally suppose that the angular flux moments decrease sufficiently rapidly

$$\sigma_\beta^{p\to q}\psi^p(r,\mu) \cong \sum_{l=0}^{L}\frac{2l+1}{4\pi}\sigma_\beta^{p\to q}P_l(\mu)\phi_l^p(r)\,, \tag{15}$$

we obtain a multigroup problem with modified total cross-section $\tilde{\sigma}_t^q$ and scattering harmonics $\tilde{\sigma}_{s,j}^{p\to q}$ for group transitions

$$\tilde{\sigma}_t^q = \sigma_{t,CSD}^q + \frac{2\beta_{q+1/2}}{\Delta E_q}, \qquad \tilde{\sigma}_{s,j}^{p\to q} = \sigma_{s,j,CSD}^{p\to q} + \frac{(-1)^{q-p+1}2(\beta_{q-1/2}+\beta_{q+1/2})}{\Delta E_q}, \quad p<q\,. \tag{16}$$

The cross-sections defined by Eqs. (12) and (16) are used in the CEPXS/ONELD package [1] as a default option. Approximations (12) and (15), used in indirect treatment of the CSD and continuous scattering operators, also define the main limitations of this approach.

Due the large values of the modified total cross-sections $\tilde{\sigma}_t^q$ (16), it is natural to use nodal schemes for approximation of the transport equation received in indirect approach. The family of nodal WLM-WLD schemes for plane geometry case can be obtained [13] by adding to the zeroth and first order balance equations for a cell $\left[x_{i-1/2}, x_{i+1/2}\right]$

$$\left(\psi_x^+ - \psi_x^-\right)\big/h + \psi^{(0)} = S^{(0)}\big/\sigma\,, \qquad 3\left(\psi_x^+ + \psi_x^- - 2\psi^{(0)}\right)\big/h + s\psi^{(1)} = sS^{(1)}\big/\sigma\,, \quad s=\mathrm{sign}(\mu)\,, \tag{17}$$

where

$$h=\frac{\sigma\Delta x_i}{|\mu_m|}, \quad \psi_{i,m}^{(k)} = \frac{2k+1}{\Delta x_i}\int_{x_{i-1/2}}^{x_{i+1/2}}\psi_m(x)p_{i,k}(x)dx\,, \quad S_{i,m}^{(k)}=\ldots, \quad p_{i0}=1, \quad p_{i1}=\frac{2}{\Delta x_i}\left(x-x_i\right), \quad k=0,1,$$

the auxiliary equation

$$\psi_x^+ = (1-P)\psi^{(0)} + (Q+P)s\psi^{(1)} + P\psi_x^-, \qquad 0\le P\le 1,\ Q=1 \text{ or } P=1,\ 1/3\le Q<\infty\,. \tag{18}$$

Here P and Q are the weighting coefficients. For the forth order of accuracy LM/QC scheme $P=Q=1$, and for the third order of accuracy LD scheme $P=0$, $Q=1$. By an appropriate choice of the weighting coefficients it is possible to ensure positivity of the scheme. In the adaptive WLM-WLD scheme [13] the weighting coefficients are chosen in result of estimation of the first and second spatial derivatives of the flux in a cell. The LM/QC, LD and AWLM-WLD schemes and the P_1SA scheme for acceleration of inner iterations convergence, consistent with the WLM-WLD scheme [14], are available in ROZ-6.5 code.

In solving problems with monodirectional sources the uncollided flux and the first-collission source are usually calculated by analytical formulas. For example, if the left boundary of a slab is illuminated by a wide monodirectional beam of radiation in angular cosine $\mu_0 = Cos\theta_0 > 0$

$$f^q_{mono}(\mu) = F^q \delta(\mu - \mu_0), \tag{18}$$

the zeroth and first spatial moments of the uncollided flux in a cell are calculated by formulas:

$$\psi^{(0),q}_{i,uncol.} = F^q a_i \frac{sh(u_i)}{u_i},\ \psi^{(1),q}_{i,uncol.} = F^q a_i \frac{3}{u_i}\left(-ch(u_i) + \frac{sh(u_i)}{u_i}\right),\ a_i = \exp\left\{-\int_{x_{int}}^{x_i} \frac{\sigma^q_t(x)dx}{\mu_0}\right\},\ u_i = \frac{\sigma^q_t \Delta x_i}{2\mu_0}, \tag{19}$$

If the CSD term is treated directly, a more complicated algorithm (similar to described in [4]) to calculate the extended uncollided flux that takes into account the CSD term is used. The main restriction of this algorithm is the need to use sufficiently fine mesh to have a possibility to take out exponent with the optical path, calculated along characteristic, from integral over a cell in the center of a cell.

5. PROBLEM OF ACCELERATION OF INNER ITERATIONS CONVERGENCE

The acceleration of inner iterations convergence in electron transport calculations is a difficult finally unresolved problem. For plane geometry problems with highly anisotropical scattering the spectral radius of the P_1SA scheme is defined by the following formula [15]:

$$\rho = \sigma_{s,2} / \sigma_t \tag{20}$$

The variant of the consistent P_1SA scheme that can be applied to the scattering low, defined by a scattering matrix, is developed in [16]. In the case of the three-diagonal Fokker-Planck (FP) scattering matrix (7) similar analyses gives:

$$\rho = \tilde{\sigma}_{s,2} / \sigma_t, \qquad \tilde{\sigma}_{s,2} = \frac{5}{2}\sum_{m,m'} w_m w_{m'} P_2(\mu_m) P_2(\mu_{m'}) T_{m,m'} \tag{21}$$

Standard P_L approximation of the FP scattering is given by Eq. (12), where $\sigma^q_{t,BFP} = \sigma^{q\to q}_{sl,BFP} = 0$. For this approximation $\sigma_{s,L} = 0$. *Optimal* P_L approximation of the FP scattering for which the value $\sigma_{s,2}/\sigma_t$ is minimized is given by [15]:

$$\sigma'_{s,l} = \sigma_{s,l} - 0.5\left(\sigma_{s,2} + \sigma_{s,L}\right), \qquad l = 0,1,\ldots,L, \tag{5.4}$$

where $\sigma_{s,l}$ are the P_L coefficients of the standard approximation.

From Figure 1 it is possible to conclude that in the case of the FP scattering the performance of the P_1SA scheme in 1D geometries degrades if the P_L approximation or quadrature order (if the FP scattering matrix is used) are increased. In 2D and 3D geometries the P_1SA scheme becomes unstable if $\sigma_{s,1} > 0.5\sigma_{s,0}$.

It seems that a direct treatment of the BFP equation opens a way for construction of a hybrid algorithm where the direct method [9] is used to partially invert the FP scattering matrix, generated by the continuous-scattering term (or by the singular part of scattering), and the consistent P_1SA scheme is used to iteratively invert the regular part of scattering.

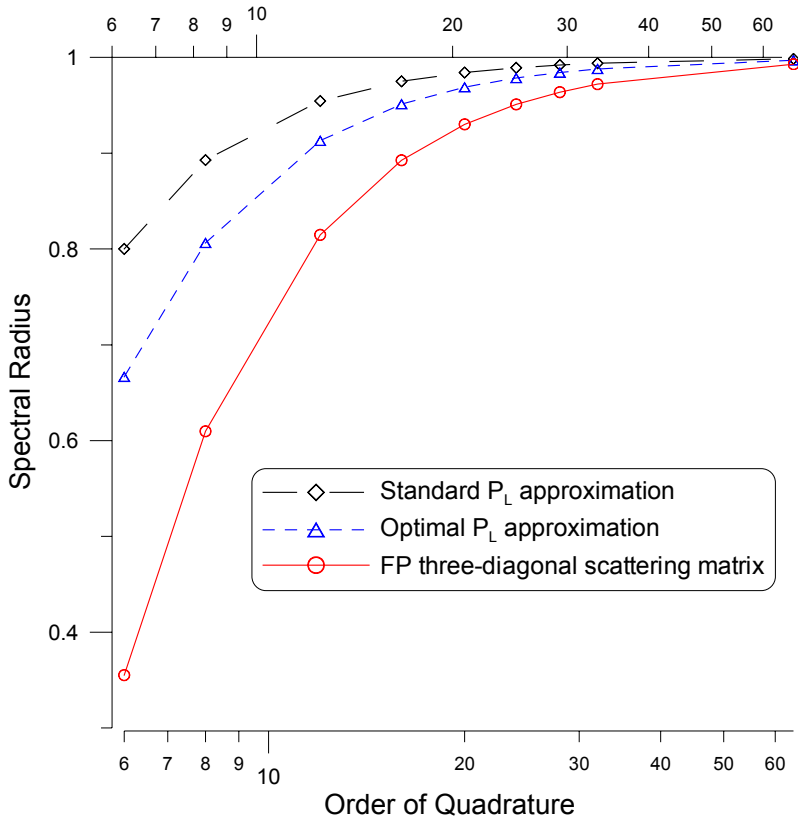

Figure 1. Spectral radius of the P_1SA scheme in dependence of approximation of the FP scattering.

6. NUMERICAL EXAMPLES

In Figures 2-7 results of calculation by the CEPXS-BFP/ROZ-6.5 package of the energy and charge deposition profiles for the sample problem from [1, 3], where 1.0 MeV electrons are normally-incident on a slab of aluminum approximately one range thick (0.2107 cm), are depicted in comparison with the CEPXS/ONELD package results. Calculations have been performed with the use of the BFP, CSD and indirect options of the CEPXS-BFP for different spatial and energy meshes, and a few differencing schemes available in ROZ-6.5 code. In ROZ-6.5 calculations (except specially noted) the uncollided flux was treated analytically. In ONEDANT-LD calculations the "normal" option was used, where no uncollided flux was selected.

To calculate the energy deposition profiles in the case of both the CSD and BFP options the following formula was used [5]:

$$D_E(\vec{r}) = \sum_{q=1}^{Q} \Sigma_E^q \Phi^q(\vec{r}) + E_{Q+1/2}\beta_{Q+1/2}\Phi_{Q+1/2}(\vec{r}),$$

where Σ_E^q and $\Phi^q(\vec{r})$ are the energy deposition cross-sections (kerma-factors) for group q; $\beta_{Q+1/2}$ and $\Phi_{Q+1/2}(\vec{r})$ are the restricted stopping power and scalar flux for the lower electron energy bound $E_{Q+1/2}$. The charge deposition profiles were calculated by formula [5]

$$D_C(\vec{r}) = \sum_{q=1}^{Q} \Sigma_C^q \Phi^q(\vec{r}) + \beta_{Q+1/2}\Phi_{Q+1/2}(\vec{r}),$$

where Σ_C^q is the charge deposition cross-section for group *q*.

From Figures 2-7 we can conclude that the use of the LD scheme with the indirect option is a good practical choice if the energy mesh is sufficiently fine [3] to suppress oscillatory nature of the DD scheme used for approximation of the CSD term. The use of the forth order of accuracy LM/QC scheme with the indirect option produces oscillations those can be suppressed by a fix-up algorithm used in the AWLM-WLD scheme. Unfortunately, the final general form of this fix-up algorithm is not still available.

The use of the AWDD scheme with direct BFP and CSD options gives acceptable results if the sufficiently fine spatial mesh is used. In this approach the fix-up algorithm is used both in spatial and energy variables and oscillatory nature of the DD scheme is suppressed in this case. The approximate algorithm for calculation of the uncollided flux, used with direct options in ROZ-6.5, requires sufficiently fine spatial mesh in the region where uncollided flux is essential. But if the quadrature order is sufficiently high the analytical treatment of the uncollided flux is not needed.

In Figures 8 and 9 results of calculation by the CEPXS-BFP/ROZ-6.5 package of spectra and energy angular distributions of the bremsstrahlung photons, emitted from the copper slabs 1.3 and 6.5 g/cm^2 thick those are bombarded by a wide normally-incident beam of 300.0 MeV electrons are presented. In these calculations 60 electron and 60 photon groups with the same energy mesh have been used. Results are normalized per 1 incident electron. The use of the optimized group sequence and upscattering iteration cycles gives the multifold computational gain in solving this problem.

CONCLUSIONS

The use of standard S_n codes, developed for neutral particle transport calculations, for charged particle transport calculations is desirable, but it is limited by the nature of the problem solved. The main special features of the coupled neutral-charged particle transport calculations are:

1. Standard group sequence and iteration cycles should be changed to receive optimal performance in solving cascade problems.
2. The direct treatment both of the CSD and continuous scattering terms, and the use of the nodal schemes for approximation both the streaming and CSD terms of the BFP equation are desirable. The use of approximations (12) and (15) those are typical for indirect approach can generate essential computational errors in some problems [4].
3. The direct treatment of the continuous scattering term of the BFP equation opens a way both to improve angular flux distributions and to construct of a hybrid algorithm where the direct method is used to partially invert the FP scattering matrix, generated by this term, and the consistent P_1SA scheme is used to iteratively invert the regular part of scattering.

So, maybe, more attractive way is a modification of S_n solvers to BFP S_n solvers by developing the BFP routines that make the same job for the BFP equation groups as the available Boltzmann routines for the Boltzmann transport equation groups.

ACKNOWLEDGEMENTS

This work was performed, in part, under auspices of the Russian Foundation for Basic Research, grant No. 01-01-00570.

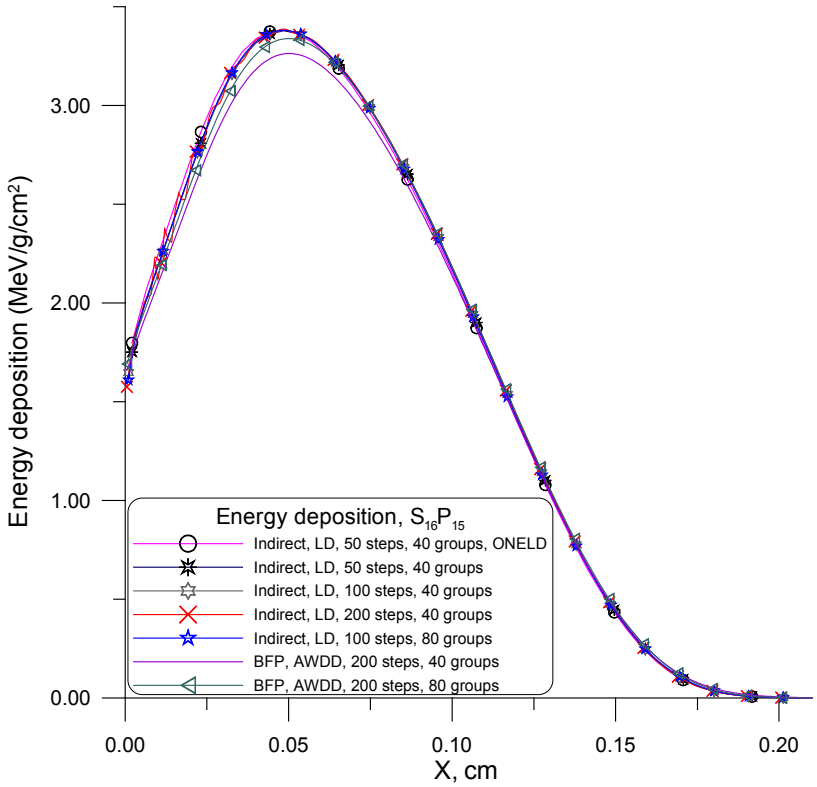

Figure 2. Energy deposition profile in aluminum slab 0.2107 cm thick, illuminated by the normally-incident 1.0 MeV electrons, calculated by means of the indirect LD and direct BFP/AWDD options.

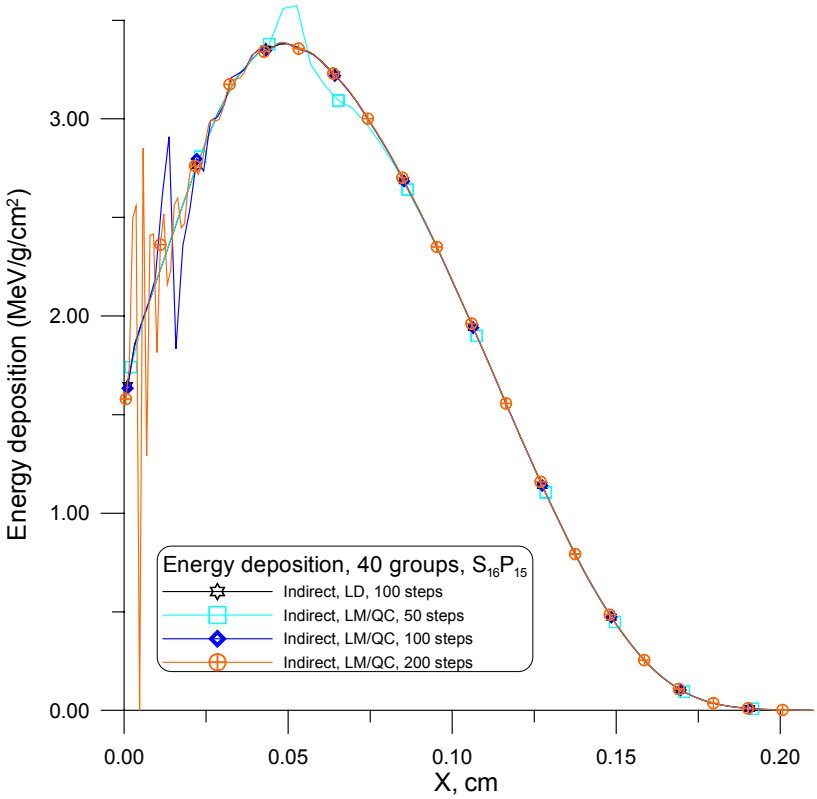

Figure 3. Energy deposition profile in aluminum slab 0.2107 cm thick, illuminated by the normally-incident 1.0 MeV electrons, calculated by means of the indirect LM/QC and LD options.

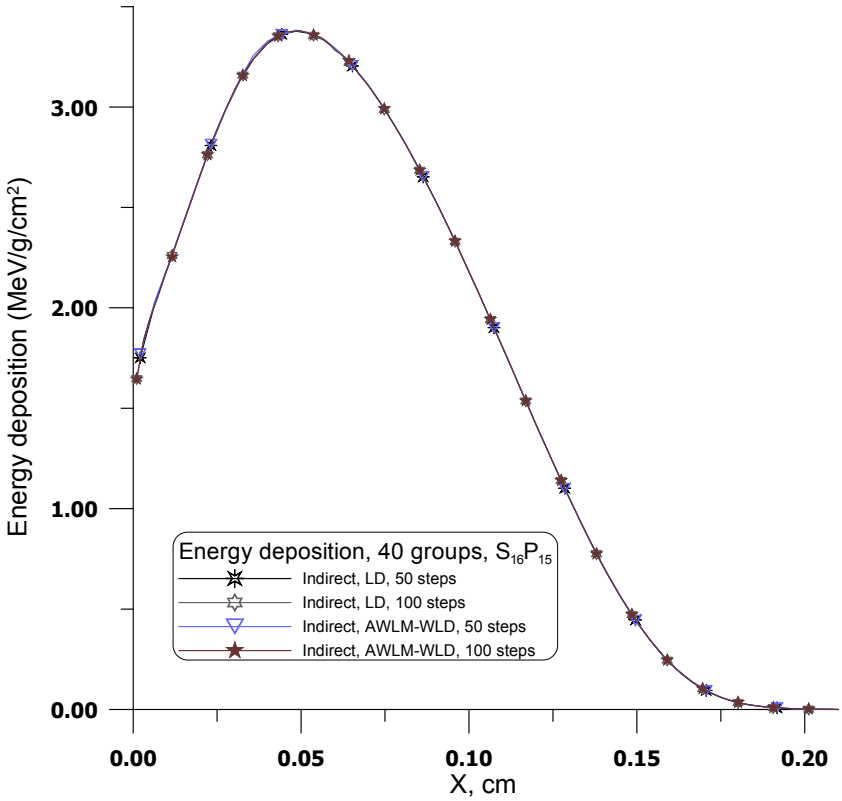

Figure 4. Energy deposition profile in aluminum slab 0.2107 cm thick, illuminated by the normally-incident 1.0 MeV electrons, calculated by means of the indirect AWLM-WLD and LD options.

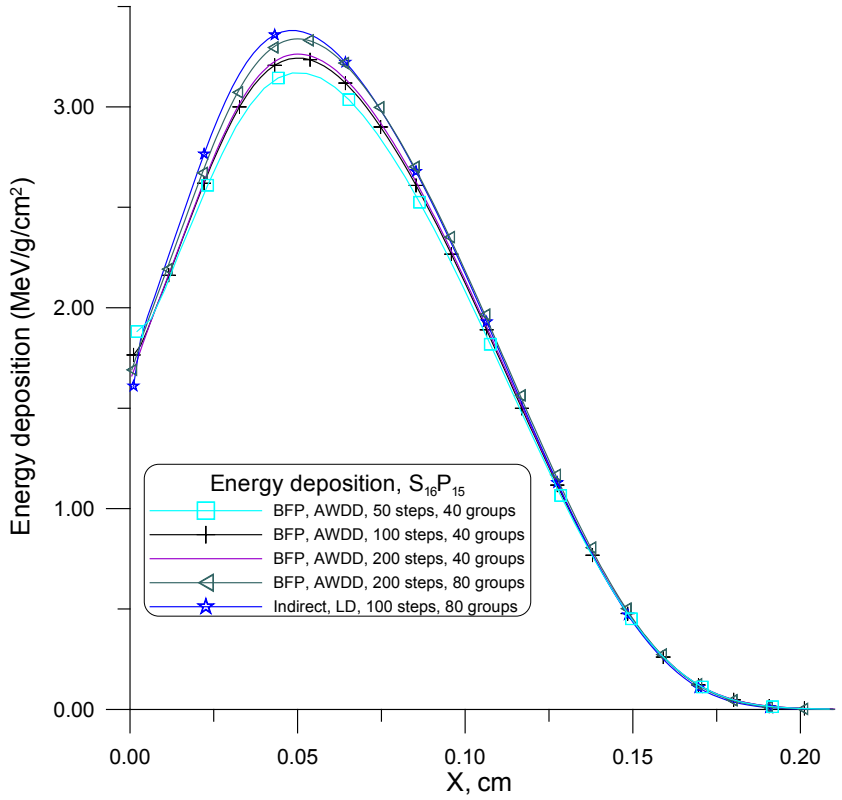

Figure 5. Energy deposition profile in aluminum slab 0.2107 cm thick, illuminated by the normally-incident 1.0 MeV electrons, calculated by means of the indirect LD and direct BFP/AWDD options.

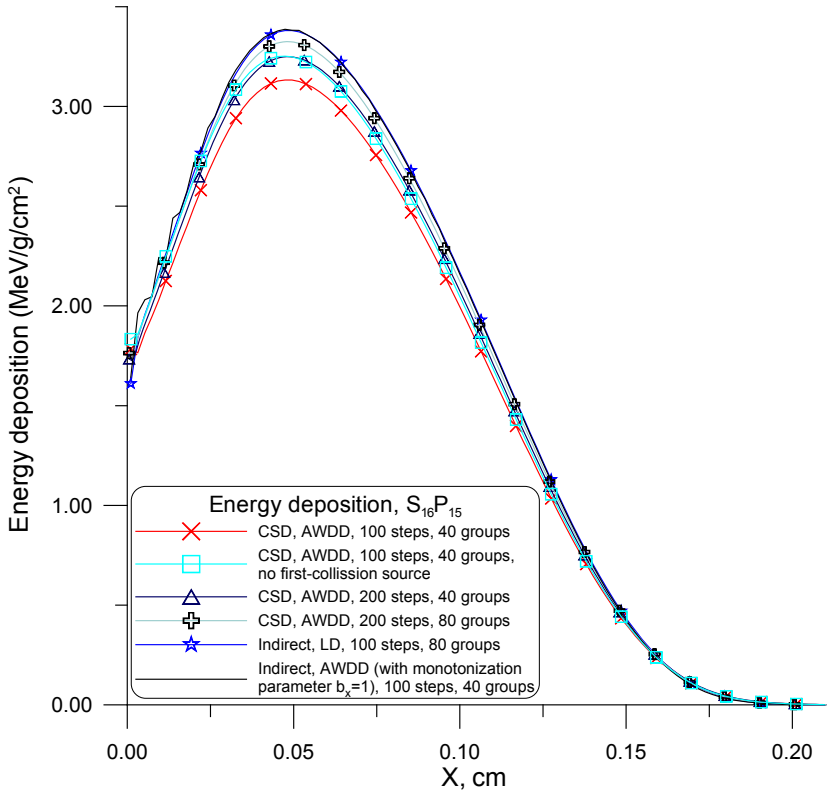

Figure 6. Energy deposition profile in aluminum slab 0.2107 cm thick, illuminated by the normally-incident 1.0 MeV electrons, calculated by the indirect LD, AWDD and direct CSD/AWDD options.

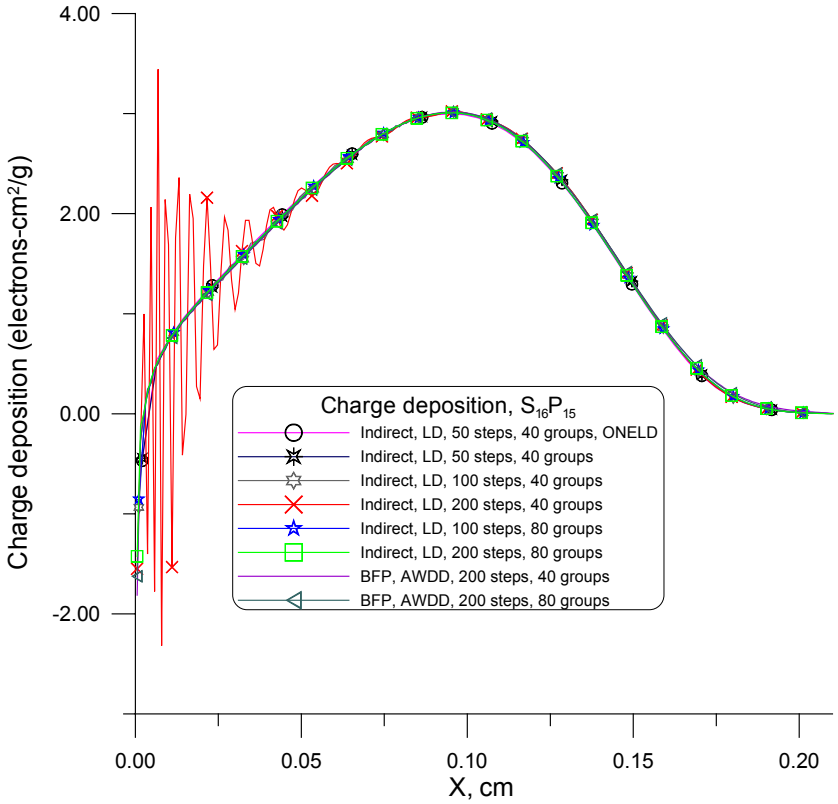

Figure 7. Charge deposition profile in aluminum slab 0.2107 cm thick, illuminated by the normally-incident 1.0 MeV electrons, calculated by means of the indirect LD and direct BFP/AWDD options.

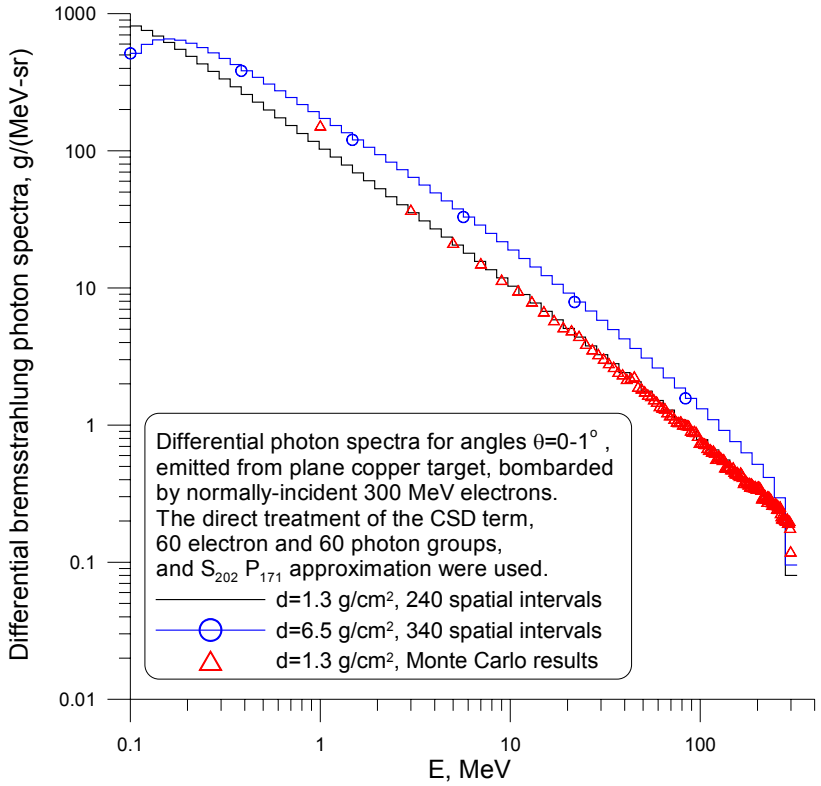

Figure 8. The differential bremsstrahlung spectra, emitted from the copper slab 1.3 and 6.5 g/cm^2 thick in the angular interval $0-1^\circ$ that is bombarded by normally-incident 300 MeV electrons.

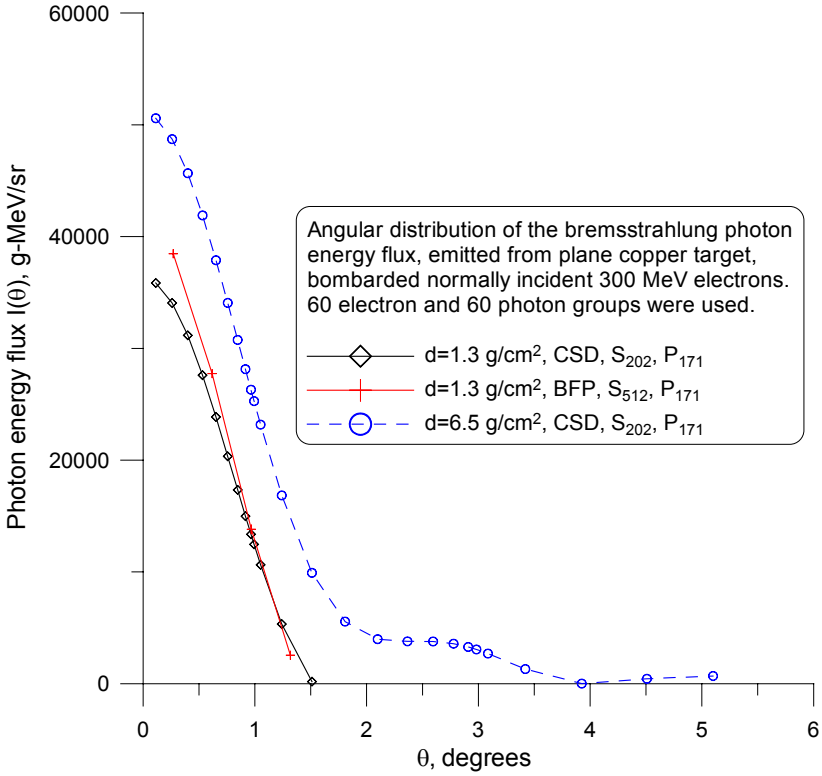

Figure 9. Angular distribution of the bremsstrahlung photons energy, emitted from the copper slabs 1.3 and 6.5 g/cm^2 thick that is bombarded by normally incident 300.0 MeV electrons.

REFERENCES

1. L. J. Lorence, Jr., J. E. Morel and G. D. Valdez, "User's Guide to CEPXS/ONELD: A One-Dimensional Coupled Electron-Photon Discrete Ordinates Code Package," Version 1.0, SAND89-1661, Sandia National Laboratories (1989).
2. L. J. Lorence, Jr., J. E. Morel and G. D. Valdez, "Physics Guide to CEPXS: A Multigroup Coupled Electron-Photon Cross-Section Generating Code," Version 1.0, SAND89-1685, Sandia National Laboratories (1989).
3. L. J. Lorence, Jr., J. E. Morel and G. D. Valdez, "Results Guide to CEPXS/ONELD: A One-Dimensional Coupled Electron-Photon Discrete Ordinates Code Package," Version 1.0, SAND89-2211, Sandia National Laboratories (1989).
4. A. M. Voloschenko, "An S_n Algorithm for Spallation Target Neutronics and Shielding Calculations," *Proc. of International Conference on Mathematics and Computations, Reactor Physics, and Environmental Analyses in Nuclear Applications*, 27-30 September, 1999, Madrid, Spain, vol. 2, p. 975.
5. J. E. Morel, L. J. Lorence, Jr., R. P. Kensek, J. A. Halbeib, D. P. Sloan, "A Hybrid Multigroup/Continuous-Energy Monte Carlo Method for Solving the Boltzmann-Fokker-Planck Equation," *Nucl. Sci. Eng.,* **124**, 369 (1996).
6. A. V. Averin, A. M. Voloschenko, E. P. Kondratenko, A. A. Dubinin, "The ROZ-6.4 One-Dimensional Discrete Ordinates Neutrons, Gamma-Rays and Charged Particles Transport Code," *Proc. Int. Topical Meeting on Advances in Mathematics, Computations and Reactor Physics*, April 28 - May 2, 1991, Pittsburgh, USA, vol. 5, p. 30.3 5-1.
7. A. M. Voloschenko and A. V. Shwetsov, "The KASKAD-1 Two-Dimensional Discrete Ordinates Nodal Transport Code," ibid., p. 30.3 4-1.
8. A. M. Voloschenko, "An Experience in the Use of the S_n Method for Hadron and Electron-Photon Transport Problems in Boltzmann-Fokker-Planck Formulation," Proc. of short course "Neutron and Radiation Transport Simulation: Theory and Applications," ed. by Prof. Nam Zin Cho, KAIST, Taejon, Korea, February 19-22, 2001, p. 319.
9. K. Przybylski, J. Ligou, "Numerical Solution of the Boltzmann Equation Including Fokker-Plank Terms," *Nucl. Sci. Eng.*, **81**, 92 (1982).
10. J. E. Morel, "An Improved Fokker-Planck Angular Differencing Scheme," *Nucl. Sci. Eng.,* **89,** 131 (1985).
11. A. M. Voloschenko, T. A. Germogenova, "Numerical Solution of the Time-Dependent Transport Equation with Pulsed Sources," *Transp. Theory and Stat. Phys*., **23**, No. 6, 845, 1994.
12. M. Landesman, J. E. Morel, "Angular Fokker-Planck Decomposition and Representation Techniques," *Nucl. Sci. Eng.*, **103**, 1 (1989).
13. A. M. Voloschenko, "Geometrical interpretation of family of weighted nodal schemes and adaptive positive approximations for transport equation, " *Proc. Joint International Conference on Mathematical Methods and Supercomputing for Nuclear Applications*, October 6-10, 1997, Saratoga Springs, NY USA, vol. 2, p. 1517.
14. A. M. Voloschenko and E. P. Kondratenko, "The KP_1 Scheme of Acceleration of Inner Iterations Convergence for Transport Equation in One-Dimensional Geometries, Consistent with the WLM-WLD Scheme," *Preprint of the Keldysh Institute of Applied Mathematics,* No. 197, 1987.
15. J. E. Morel, T. A. Manteuffel, "An angular multigrid acceleration technique for S_n equations with highly forward-peaked scattering," *Nucl. Sci. Eng.,* **107**, 330 (1991).
16. A. M. Voloschenko, "Completely Consistent P_1 Synthetic Acceleration Scheme for Charged-Particle Transport Calculations," *Proc. 1996 Top. Meet. Radiation Protection and Shielding*, April 21-25, 1996, No. Falmouth, Massachusetts, vol. 1, p. 408.